

Supplemental Material

Interactions of the KWK₆ Cationic Peptide with Short Nucleic Acid Oligomers:
Demonstration of Large Coulombic End Effects on Binding at 0.1–0.2 M Salt

Jeff D. Ballin*, Irina A. Shkel* and M. Thomas Record, Jr.*, †
Departments of Chemistry* and Biochemistry†
University of Wisconsin-Madison
Madison, WI 53706 U.S.A.

Materials and Methods Supplemental Information

Buffers. Salt cation concentrations reported in this study include contributions from the buffer. For example, the 0.1 M Na⁺ titrations contained 0.2 mM Na₂EDTA, 5 mM sodium cacodylate pH 6.0, and 95 mM NaOAc; the 35 mM Na⁺ titrations contained 0.2 mM Na₂EDTA, 5 mM sodium cacodylate pH 6.0, and 30 mM NaOAc, etc. These conditions were obtained by mixing linear combinations of “low salt” (0.2 mM Na₂EDTA, 5 mM sodium cacodylate pH 6.0) and “high salt” (0.2 mM Na₂EDTA, 1.0 M NaOAc, 5 mM sodium cacodylate pH 6.2) buffers. The final pH of these buffer mixtures was 6.06 ± 0.03 for the tested [Na⁺] range 0.0053–0.32 M (data not shown).

Peptide synthesis and purification. Fmoc-L-Lys(Boc)-OPfp and Fmoc-L-Trp-OPfp (both from Millipore; Bedford, MA) were coupled onto a NovaSyn PR 500 PAL resin (Calbiochem-Novabiochem; San Diego, CA) in the presence of excess 1-hydroxybenzotriazole (Aldrich Chemical Company; Milwaukee, WI) in dimethylformamide (FisherBiotech; Fair Lawn, NJ), monitoring Fmoc deprotection spectroscopically. The oligopeptide was purified using a semi-preparative reverse phase Kromasil 5 μ m C₁₈ HPLC column (Technikröm; Wilmette, IL) first with a sodium phosphate-acetonitrile gradient solvent system followed by a water-acetonitrile (0.1% TFA) gradient to desalt the sample. KWK₆ elution was monitored by absorbance at 280 nm. Samples were then pooled, lyophilized, and characterized using matrix-assisted laser desorption ionization mass spectroscopy (Biochemistry Instrumentation Facility, Madison, WI).

Fluorescence titrations. All titrations were performed in siliconized quartz cuvettes to minimize the possibility of adsorption of the oligopeptide or DNA to the cuvette walls. The temperature was regulated with a VWR Scientific (South Plainfield, NJ) Model 1156 circulating water bath. To minimize photobleaching, the excitation shutters were opened only during measurement (less than a minute of sample exposure to light per measurement).

After an hour of continuous irradiation, the oligopeptides exhibited less than 3% loss in fluorescence. To correct for Raman light scattering from the water and any background fluorescence emission, the fluorescence of a buffer solution (containing no oligopeptide) at the equivalent DNA concentration in the titration was subtracted from the fluorescence signal of the sample. The photon counter for the SLM Amino fluorometer was a solution of 3 mg/ml Rhodamine B in ethylene glycol, which exhibited photobleaching under the conditions used in these experiments. To account for this effect, each data point was multiplied by the ratio of the average reference counts measured at the time of data collection versus the average reference counts measured at the time of the initial peptide fluorescence (before any DNA was added).

Ligand binding density functional analysis. LBDF analysis [1] provides a model-independent method to show that fluorescence quenching, Q_{obs} (eq. 1), is proportional to the concentration of bound peptide, $[P_B]$,

$$\frac{Q_{obs}}{Q_{max}} = \frac{[P_B]}{[P_T]}, \quad (\text{s1})$$

and thus proportional to binding density,

$$\nu = \frac{[P_B]}{[D_T]} = \left(\frac{Q_{obs}}{Q_{max}} \right) \left(\frac{[P_T]}{[D_T]} \right), \quad (\text{s2})$$

where $[P_T]$ and $[D_T]$ are the total molar concentrations of KWK₆ and of DNA phosphate, and Q_{max} , the maximum quenching, is attained when all peptide is bound (*i.e.*, when $\frac{[P_B]}{[P_T]} = 1$). Therefore, $[P_F]$ is related to $[P_T]$ from eq. s1 by

$$[P_F] = \left(1 - \frac{Q_{obs}}{Q_{max}} \right) [P_T]. \quad (\text{s3})$$

Equilibrium binding constants are determined by fitting the dependence of ν and $[P_F]$ as a function of $[L_T]$ and $[D_T]$ to a given model (see text).

Mean ionic activity calculations. Sodium acetate molarities ($[NaOAc]$) were converted to mean ionic activities (a_{\pm}) by first calculating the corresponding molalities (m_{NaOAc}) via quadratic interpolation of standard data [2] within the range of 0.060–1.1 M NaOAc:

$$\begin{aligned} m_{NaOAc} = & (0.04592 \pm 0.0003) * [NaOAc]^2 + \\ & (0.9999 \pm 0.0004) * [NaOAc] + \\ & (0.0001354 \pm 0.0000901) \end{aligned} \quad (\text{s4})$$

This calculated molality was then used to interpolate the mean activity coefficient (γ_{\pm}) at this concentration, using the fit to the extended Debye-Hückel equation obtained for NaOAc [3]:

$$\log \gamma_{\pm} = \frac{-A_m \sqrt{I_m}}{1 + B^* \sqrt{I_m}} + \beta_m I_m \quad (\text{s5})$$

where $A_m = 0.5108$ on the molality scale at 25°C , $B^* = 1.50$ and $\beta_m = 0.08732$ for sodium acetate, and I_m is the ionic strength of the solution [3]. Since the concentration of NaOAc greatly exceeds that of all other charged species in solution, I_m is set equal to the NaOAc molality. Eq. s5 with the above parameters fits the NaOAc isopiestic data [4, 5] between 0.1–0.6 molal within the uncertainties in the data. The mean ionic activity ($a_{\pm} = \gamma_{\pm} m_{\text{NaOAc}}$) of NaOAc is obtained from equations s4–s5.

Discussion Supplementary Material

Model for axial dependence of surface cation concentration Figure S6 shows NLPB results [6] calculated at 0.1 M Na^+ for a primitive cylinder model of single stranded DNA. The salt cation concentration in the vicinity of the DNA surface is very high in the interior, but falls off strongly in the terminal regions of the model DNA for all lengths considered. For example, an 80-mer ssDNA has a surface Na^+ concentration of 1.8 M at its axial center and 0.8 M Na^+ at its end when the bulk salt concentration is 0.1 M. A 10-mer ssDNA has a 1.6 M Na^+ surface concentration at its interior, but a 0.5 M concentration at its end at 0.1 M Na^+ bulk concentration. For ssDNA oligomers with no more than 20 charges (phosphates), the surface cation concentration in the interior region of DNA is predicted to increase with increasing number of phosphates (charges). Above a length of 20 phosphates, the surface cation concentration of the strand interior has the polymeric limiting value. However, as $|Z_D|$ increases, the size of this interior region with polymeric ion accumulation increases, resulting in a “trapezoidal” axial profile of the local cation concentration. These nucleic acid lengths are considered “long.” N_e , which describes the number of phosphates on either side of the plateau where the ion accumulation is decreasing towards the ends, remains fixed as the interior region increases. When the surface cation concentration in the interior region is less than the polymeric value, a DNA oligomer is defined as short; short oligomers exhibit a “parabolic” axial cation concentration distribution.

References

- [1] Lohman, T. M. and Mascotti, D. P. (1992) Nonspecific ligand–DNA equilibrium binding parameters determined by fluorescence methods. *Methods in Enzymology*, **212**, 424–458.
- [2] Weast, R. C., (ed.) CRC Handbook of Chemistry and Physics pp. D–260 CRC Press Boca Raton, FL 63rd edition (1982).
- [3] Hamer, W. J. and Wu, Y.-C. (1972) Osmotic coefficients and mean activity coefficients of uni-valent electrolytes in water at 25°C . *Journal of Physical Chemistry Reference Data*, **1**(4), 1047–1099.
- [4] Robinson, R. A. (1935) The activity coefficients of alkali nitrates, acetates, *p*-toluenesulfonates in aqueous solution from vapor pressure measurements. *Journal of the American Chemical Society*, **57**, 1165–1168.

- [5] Smith, E. R. B. and Robinson, R. A. (1942) The vapour pressures and osmotic coefficients of solutions of the sodium salts of a series of fatty acids at 25°. *Transactions of the Faraday Society*, **38**, 70–78.
- [6] Ni, H. Theoretical and Experimental Studies of Coulombic Effects of Salt on DNA Processes PhD thesis University of Wisconsin-Madison (1999).
- [7] Zhang, W., Bond, J. P., Anderson, C. F., Lohman, T. M., and Record, Jr., M. T. (1996) Large electrostatic differences in the binding thermodynamics of a cationic peptide to oligomeric and polymeric DNA. *Proceedings of the National Academy of Sciences*, **93**, 2511–2516.
- [8] Zhang, W., Ni, H., Capp, M. W., Anderson, C. F., Lohman, T. M., and Record, Jr., M. T. (1999) The importance of coulombic end effects: Experimental characterization of the effects of oligonucleotide flanking charges on the strength and salt dependence of oligocation (L^{8+}) binding to single-stranded DNA oligomers. *Biophysical Journal*, **76**, 1008–1017.

Table SI: Fitted Q_{max} binding parameters. Experimentally determined parameters for the binding affinity (and its salt dependence) of KWK₆ with dT-mers using fitted values of Q_{max} . Errors are reported with 95% confidence intervals (see *Materials and Methods*).

dT-mer	Z_D	Fitted Q_{max} (%)	$\log K_{obs}$ ([Na ⁺] = 0.105 M)	Fitted Q_{max} $-S_a K_{obs}^{\parallel}$	$\log K_0^{\parallel}$ (1 M Na ⁺)
poly dT	169*	$88 \pm 4^{\dagger\dagger}$	$6.64 \pm .70^{\S}$	$7.25 \pm .52^{**\dagger\dagger}$	$-1.20 \pm .42^{**\dagger\dagger}$
dT(pdT) ₆₉	69 [†]	$97 \pm_3^{\dagger\dagger}$	$5.91 \pm .27^{\dagger\dagger\S}$	$5.41 \pm .19$	$0.07 \pm .18$
dT(pdT) ₃₉	39 [†]	95 ± 2	$5.94 \pm .07$	$5.98 \pm .06$	$-0.29 \pm .05$
dT(pdT) ₂₂	22	95 ± 2	$5.60 \pm .05$	$5.56 \pm .16$	$-0.39 \pm .14$
dT(pdT) ₁₅	15 [†]	87 ± 5	$5.47 \pm .13$	$5.57 \pm .57$	$-0.59 \pm .55$
dT(pdT) ₁₄	14	88 ± 2	$5.32 \pm .04$	$5.91 \pm .91$	$-1.08 \pm .88$
dT(pdT) ₁₁	11	85 ± 2	$4.92 \pm .02$	$4.51 \pm .05$	$0.00 \pm .03$
dT(pdT) ₁₀	10*	90 ± 1	$4.72 \pm .02$	$3.96 \pm .15$	$0.34 \pm .14$
dT(pdT) ₆	6	$81 \pm 2^{\ddagger}$	$3.45 \pm .28^{\S}$	$3.00 \pm .15^{\parallel}$	$0.20 \pm .23^{\parallel}$

*Saltback data [7] reanalyzed within the range considered here.

[†]Saltback data [8] reanalyzed within the range considered here.

[§]Linearly extrapolated to 0.105 M [Na⁺] using eq. 6.

[‡] Q_{max} value for dT(pdT)₆ at 0.035 M [Na⁺]. dT(pdT)₆ at 0.015 M [Na⁺] has $Q_{max} = 80 \pm 2\%$.

[¶]Two point determination of $S_a K_{obs}$ and $\log K_0$. $\log K_{obs} = 4.76 \pm 0.03$ at 0.035 M Na⁺ and $\log K_{obs} = 5.78 \pm 0.04$ at 0.015 M Na⁺. Errors in $\log K_{obs}$ are propagated to determine error.

^{||} $S_a K_{obs}$, SK_{obs} and $\log K_0$ were determined within $0.083 M \leq a_{\pm} \leq 0.19 M$ (0.105 – 0.25 M [Na⁺]) unless otherwise indicated.

^{**} $S_a K_{obs}$, SK_{obs} and $\log K_0$ were determined within $0.15 M \leq a_{\pm} \leq 0.19 M$ (0.195 – 0.25 M [Na⁺]).

^{††}Values determined at 0.196 M [Na⁺] because binding is too tight at 0.106 M [Na⁺] for accurate estimation.

^{‡‡}Fitting with floated parameters for 0.106 M [Na⁺] data did not converge.

Table SII: Constrained common intersection point binding parameters. Experimentally determined parameters for the salt dependence of KWK_6 with dT-mers using LBDF values of Q_{max} , where all fits are constrained to intersect at a single point. The salt range considered was $0.083 M \leq a_{\pm} \leq 0.19 M$ ($0.105 - 0.25 M [Na^+]$) unless otherwise specified. Fits are shown in Figures 2B and S4B. The common intersection point has a $\log K_{ref} = 1.89 \pm 0.20$ at $a_{ref} = 0.403 \pm 0.041M$ when fit on a mean activity scale and $\log K_{ref} = 1.89 \pm 0.20$ at $[Na^+]_{ref} = 0.55 \pm 0.07M$ on the concentration scale.

dT-mer	Z_D	$-SK_{obs}$	$\log K_0$ (1 M a_{\pm}) [§]	$-S_a K_{obs}$	$\log K_0$ (1 M $[Na^+]$) [‡]
poly dT* [¶]	169	6.37 ± 0.31	0.26 ± 0.43	$6.73 \pm .30$	$-0.76 \pm .38$
dT(pdT) ₆₉ [†]	69	6.22 ± 0.34	0.30 ± 0.42	$6.23 \pm .20$	$-0.56 \pm .35$
dT(pdT) ₃₉ [†]	39	5.73 ± 0.18	0.42 ± 0.39	$6.05 \pm .19$	$-0.49 \pm .34$
dT(pdT) ₂₂	22	5.14 ± 0.11	0.57 ± 0.36	$5.43 \pm .12$	$-0.25 \pm .31$
dT(pdT) ₁₅ [†]	15	4.66 ± 0.06	0.70 ± 0.34	$4.92 \pm .06$	$-0.05 \pm .29$
dT(pdT) ₁₄	14	4.48 ± 0.21	0.74 ± 0.33	$4.73 \pm .21$	$0.03 \pm .27$
dT(pdT) ₁₁	11	4.11 ± 0.08	0.84 ± 0.31	$4.34 \pm .09$	$0.18 \pm .27$
dT(pdT) ₁₀ [*]	10	3.81 ± 0.10	0.91 ± 0.30	$4.03 \pm .10$	$0.30 \pm .27$

*Ref. [7].

†Ref. [8].

‡Linearly extrapolated to 1 M $[Na^+]$ (a_{\pm}) using $\log K_0 = \log K_{ref} - (S_a K_{obs}) \log a_{ref}$.

§Linearly extrapolated to 1 M $[Na^+]$ using $\log K_0 = \log K_{ref} - (SK_{obs}) \log [Na^+]_{ref}$.

¶Fit range was $0.15 \leq a_{\pm} \leq 0.19$ ($0.195 \leq [Na^+] \leq 0.25$).

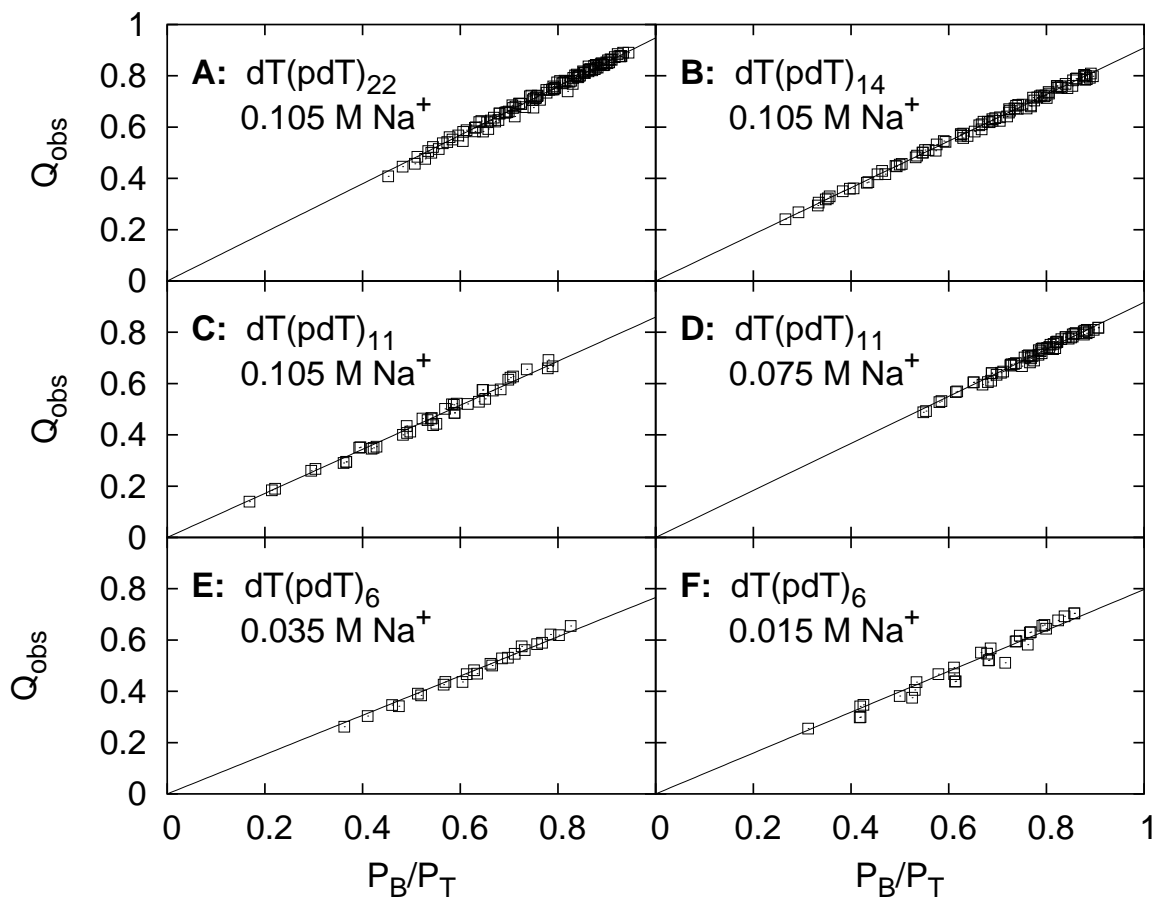


Figure S1: LBDF Analysis to obtain Q_{max} from plots of corrected fluorescence quenching (Q_{obs}) plotted versus the ratio of bound versus total oligopeptide ($[P_B]/[P_T]$) for KWK₆ to binding to varying lengths of dT-oligomers: (A) dT(pdT)₂₂ at 0.105 M Na⁺, (B) dT(pdT)₁₄ at 0.105 M Na⁺, (C) dT(pdT)₁₁ at 0.105 M Na⁺, (D) dT(pdT)₁₁ at 0.075 M Na⁺, (E) dT(pdT)₆ at 0.035 M Na⁺, and (F) dT(pdT)₆ at 0.015 M Na⁺. All determinations were performed at pH 6.0 and 25 °C. Values for the maximum fluorescence quenching (Q_{max}) obtained from extrapolation to $[P_B]/[P_T] = 1$ are listed in Table I. DNA concentration ranges are (A) 0.6–80 μ M, (B) 5–120 μ M, (C) 9–140 μ M, (D) 20–100 μ M, (E) 20–100 μ M, (F) 4–33 μ M. KWK₆ concentration ranges are (A) 0.5–3 μ M, (B) 0.4–2 μ M, (C) 0.6–1.4 μ M, (D) 1.7–3.4 μ M, (E) 0.9–1.5 μ M, (F) 1.0–1.9 μ M.

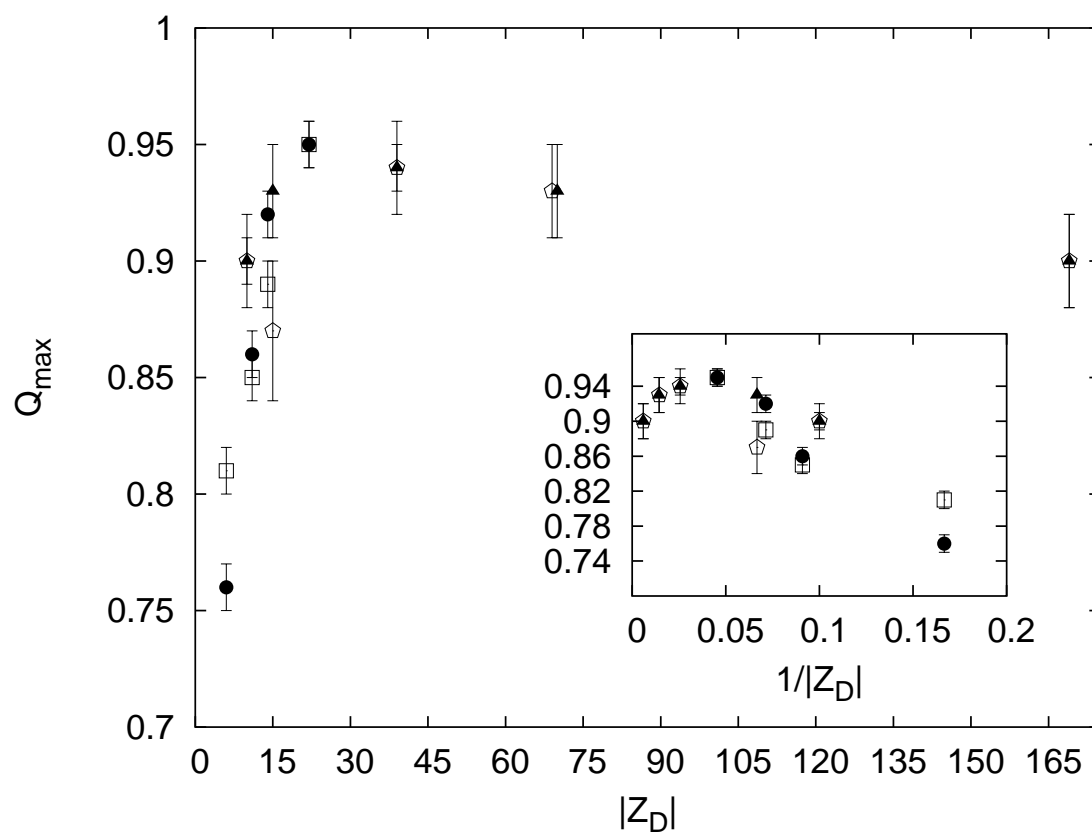


Figure S2: Dependence of Q_{max} on Number of DNA charges. The maximum fluorescence quenching, Q_{max} , of KWK₆ plotted versus oligonucleotide charge, $|Z_D|$. Values were determined via LBDF analysis (black diamonds for current work or black circles for Zhang et al. [8]) or nonlinear least squares fitting (open pentagons, current work; open squares, Zhang et al. [8]).

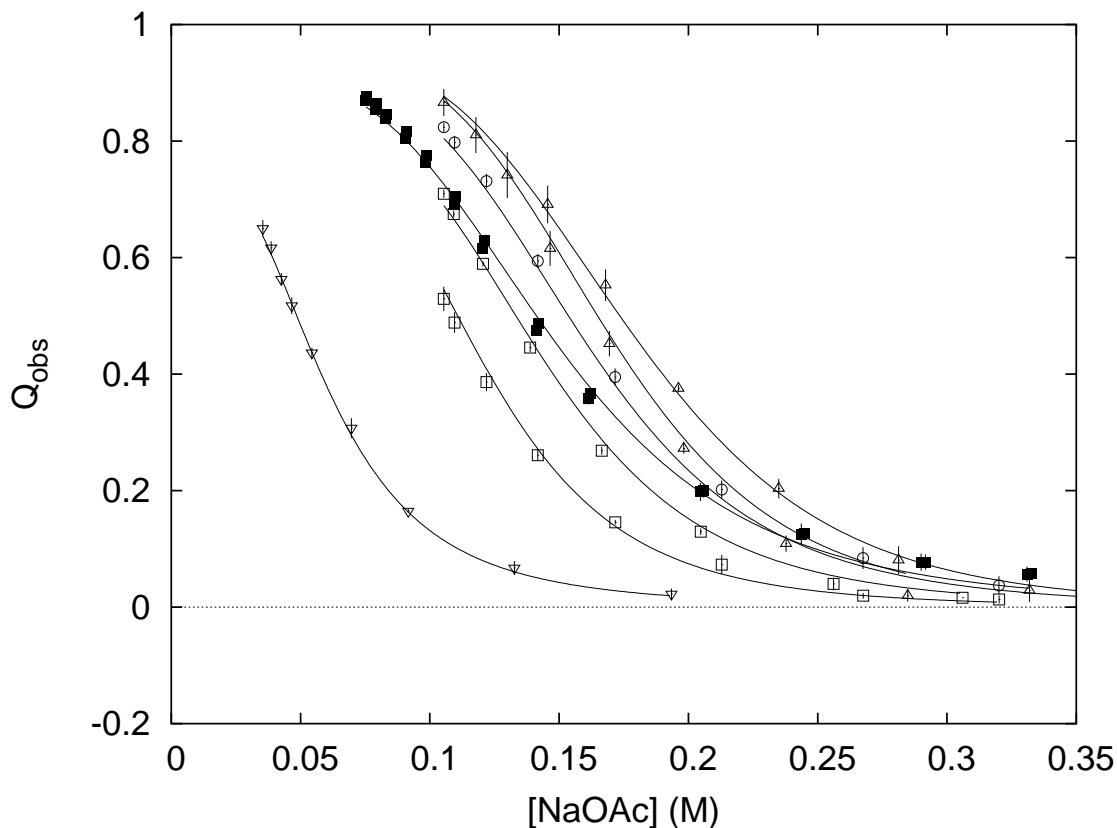


Figure S3: Saltback Titrations. Reduction in fluorescent quenching with increasing salt concentration during the saltback titration for each of the oligo-dT DNA lengths. dT(pdT)₂₂ (open triangles) where D_T ([DNA phosphate]) 81–42 μM or 77–56 μM , dT(pdT)₁₄ (open circles) where D_T 0.14 mM –80 μM , dT(pdT)₁₁ at 0.105 M Na⁺ (open squares) where D_T 0.15–0.12 mM or 68–51 μM , and dT(pdT)₁₁ (black squares) at 0.075 M Na⁺ where D_T 0.19–0.14 mM. The error bars show the variation in the average Q_{obs} for all ligand concentrations of the reverse titrations shown in Figure 1. Additional titrations for dT(pdT)₁₁ at 0.105 M Na⁺ (open squares) and dT(pdT)₂₂ at 0.105 M Na⁺ (open triangles) represent saltbacks started at two different DNA concentrations listed above. For both dT(pdT)₁₁ and dT(pdT)₂₂, the DNA concentration range listed first is associated with the higher Q_{obs} dataset.

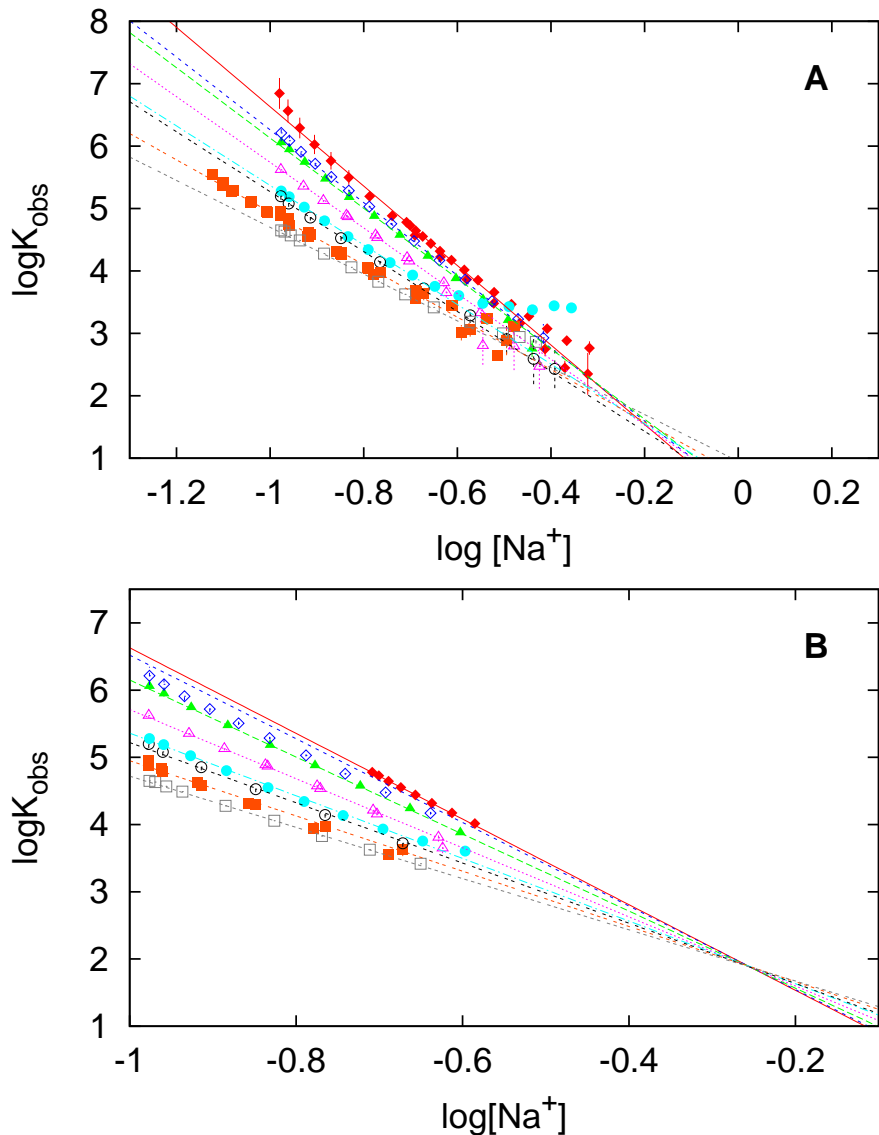


Figure S4: $S_a K_{obs}$ Analysis. Log-log plot of K_{obs} versus concentration of NaOAc for KWK₆ binding to poly-dT (red diamonds), dT(pdT)₆₉ (open blue diamonds), dT(pdT)₃₉ (green triangles), dT(pdT)₂₂ (open purple triangles), dT(pdT)₁₅ (light blue circles), dT(pdT)₁₄ (open black circles), dT(pdT)₁₁ (orange squares), and dT(pdT)₁₀ (open grey squares). The lines represent the least squares linear fits of the data between 0.1 M–0.25 M NaOAc using the parameters summarized in Table SI in Panel A, where each DNA length was fit separately. Panel B shows the subset of data from panel A fit globally to intersect at a single point (*Cf.* Table SII).

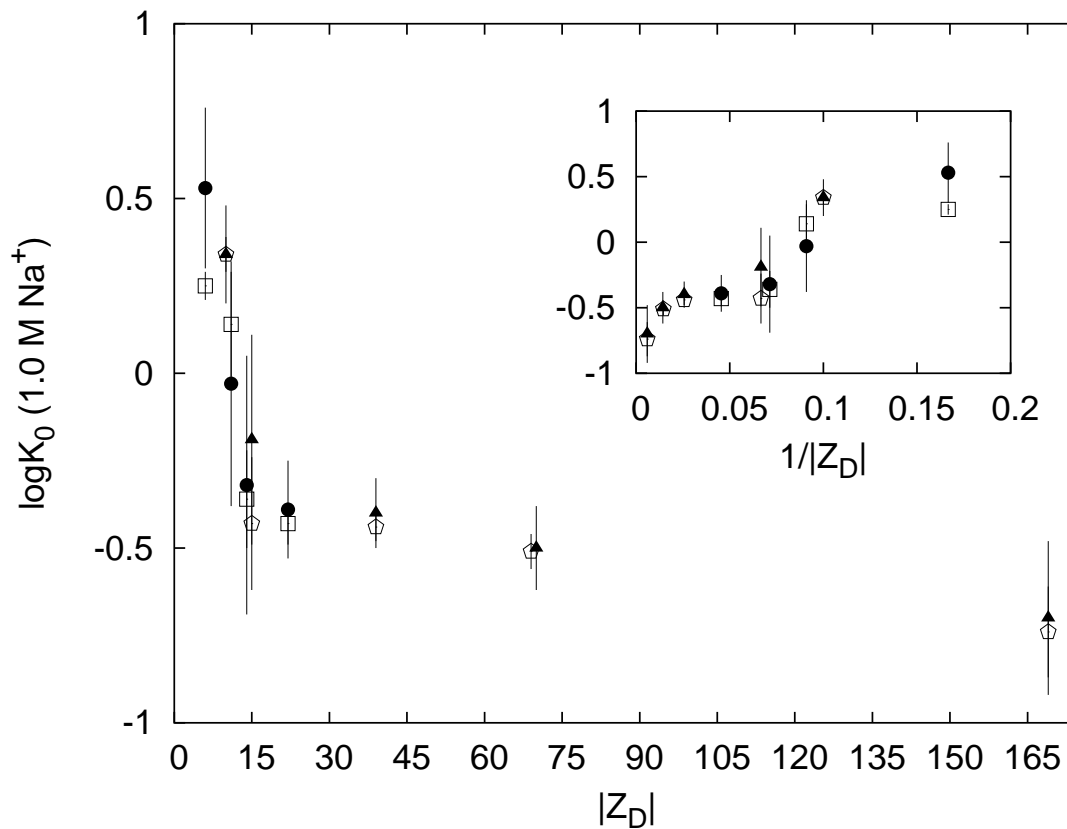


Figure S5: Dependence of $\log K_0$ (1 M salt) on Number of DNA Charges. $\log K_0$ values, determined via linear extrapolation to $a_{\pm}=1$ M $[\text{Na}^+]$ of $\log K_{obs}$ vs. $\log a_{\pm}$ data fit between 0.1–0.25 M $[\text{Na}^+]$, are plotted vs. $|Z_D|$. Results of the reanalysis of data previously published [7, 8] using either fitted (open pentagons) or LBDF (black diamonds) values of Q_{max} and from the current work (open squares and black circles for fitted vs. LBDF Q_{max} , respectively) are detailed in Tables I–SI.

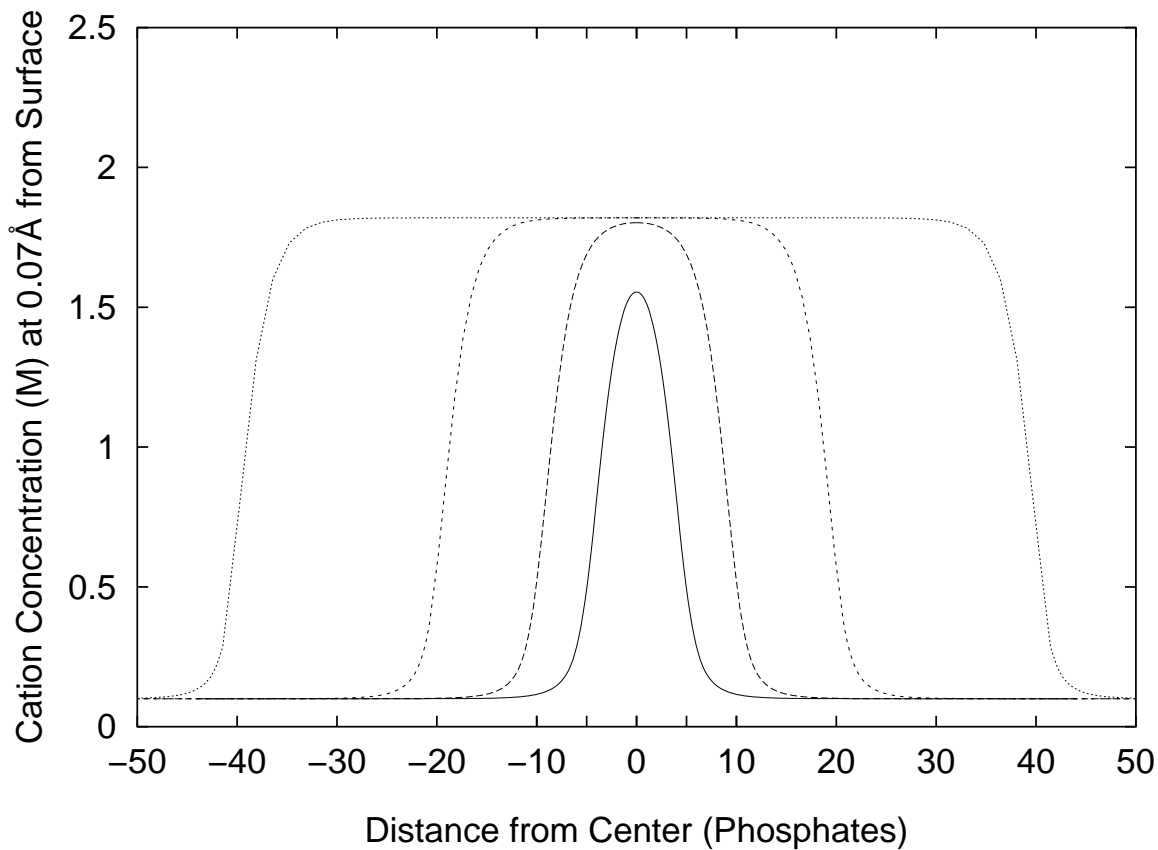


Figure S6: “Trapezoid” and “parabola” axial surface distributions of cation concentration around single-stranded DNA. NLPB calculations for ssDNA ($a=7\text{\AA}$, $b=1.7\text{\AA}$) at 0.1 M Na^+ (adapted from [6]) of different $|Z_D|=10, 20, 40,$ and 80 . The trapezoid geometry is a good approximation to the profile of the 20mer, 40mer, and 80mer, while a parabola is a good approximation for the 10mer. Note that the 20mer is at the threshold of having an interior with polymeric cation concentration.